



OPEN ACCESS

SUBMITTED 09 August 2025

ACCEPTED 15 August 2025

PUBLISHED 13 September 2025

VOLUME Vol.07 Issue 09 2025

CITATION

Banaz Mohammed Hasan. (2025). FPDCnet: A Multi-Classification Model for Classifying COVID-19, Pneumonia, and Normal Chest X-ray Imagery Using Fractional Partial Differential Algorithms. The American Journal of Applied Sciences, 7(09), 16–25.
<https://doi.org/10.37547/tajas/Volume07Issue09-03>

COPYRIGHT

© 2025 Original content from this work may be used under the terms of the creative common's attributes 4.0 License.

FPDCnet: A Multi-Classification Model for Classifying COVID-19, Pneumonia, and Normal Chest X-ray Imagery Using Fractional Partial Differential Algorithms

Banaz Mohammed Hasan

Department of Mathematics, College of Science, University of Kirkuk, Iraq

Abstract: Globally, the coronavirus (COVID-19) has had a negative impact on economies and healthcare systems. Clinical practitioners may become confused while identifying this new form of flu because the symptoms of COVID-19 are similar to those of existing chest conditions as pneumonia, tuberculosis (TB), lung cancer (LC), and pneumothorax. To address this problem, this study created a model to categorize various chest infections. In medical practice, chest x-ray examinations are the most common diagnostic technique and the main means of identifying these different types of chest infections. Researchers and paramedics are working hard to develop an accurate and reliable technique for the early diagnosis of COVID-19 to save lives; however, the diagnosis of COVID-19 remains highly idiosyncratic and varies significantly. Therefore, a multi-classification method was created and tested in this work based on deep learning (DL) and a mathematical algorithm model for automatic differentiation of COVID-19 cases from pneumonia based on chest x-ray images. These two diseases were diagnosed using a hybrid model named FPDCnet, which integrates a convolutional neural network (CNN) and Fractional Partial Differential models. This model was used alongside publicly available benchmark data to identify the diseases, and the performance was evaluated using several objective metrics, where it recorded an impressive accuracy of 98.1 %; the model

also demonstrated remarkable precision (0.982), recall (0.980), and F1-score (0.981) values.

Keywords: *COVID-19 infection; Pneumonia infection; Image classification; Chest x-rays; CNN; Fractional partial differential algorithms.*

1. Introduction

The early days of December 2019 marked the emergence of a new kind of disease in Wuhan, China, where people reported pneumonia-like symptoms with unexplained origins [1]; such patients displayed signs similar to those of severe acute respiratory syndrome (SARS). However, there were other alarming problems, and only a few persons displayed signs of a rapid progression to acute respiratory distress (ARD) [2]. Few days later, specifically on January 7, 2020, a breakthrough towards solving the rubble was announced when a patients' throat swab sample was used to identify the disease by the "Chinese Centre for Disease Control and Prevention" (CCDC); the disease was identified as a novel coronavirus (nCoV), which was later designated by the "World Health Organization" (WHO) as 2019-nCoV [3]. Since December 31, 2021, more than 284,992,606 persons have been infected by the virus, resulting in more than 5,000,000 deaths, and > 2,000,000 recoveries [4]. In severe cases, frontline specialists first needed to use the RT-PCR test to identify COVID-19 [5]. After the infected person's DNA is extracted using the reverse transcription technique, it is subjected to PCR to strengthen it before analysis. This process can detect coronavirus because it is an RNA virus [6]. The increasing demand for rapid COVID-19 test results caused significant delays in results delivery form using only PCR kits; again, most of these PCR kits produce false-negative (FN) results that makes their results unreliable [7]. The symptoms of COVID-19 infection include fever, coughing, shortness of breath, sore throat, chest pain, and loss of taste or smell. As these symptoms are also common in patients with tuberculosis (TB) and pneumonia, clinicians find it challenging to identify COVID-19. Hence, researchers and medical professionals are working to find a reliable way to diagnose COVID-19, such as methods based on X-ray image analysis [4]. These days, chest radiography, or chest x-rays, is one of the most used and affordable clinical diagnostic techniques [8] [9].

Image analysis has become one of the recent methods of detecting and diagnosing deadly illnesses like TB and pneumonia, as well as the early stages of LC [10]. A chest

X-ray can reveal a great deal about a patient's medical history. While correctly identifying COVID-19 on a chest radiograph is always a top priority for medical professionals, the overlapping tissue features in chest x-rays have significantly raised the difficulty of accurate analysis. Therefore, it is difficult for practitioners to identify COVID-19 when the lesion partially covers the ribs or closely resembles nearby tissues. It can occasionally be difficult to distinguish between COVID-19, LC, pneumonia, and TB from chest x-rays, even for a skilled medical professional. Consequently, this problem might be solved by employing artificial intelligence (AI), especially deep learning models, to automatically diagnose these illnesses from chest radiographs [11]. There has been a great deal of excitement about news that deep learning and transfer learning techniques outperform people in diagnostic assessments. In artificial intelligence, both approaches (especially deep learning) offer a framework for utilizing previously learned information to tackle novel but pertinent tasks considerably more quickly and efficiently [12]. Its ability to fine-tune based on previously trained models is a key component of the transfer learning process. Because of this feature, deep learning models are the most widely used method for disease classification from medical images. The classification of diseases has been transformed by DL models, which have also opened up new avenues for medical practitioners [13], [14]. Medical systems collaborating with CNN have made substantial advancements in disease diagnosis, such as cancer diagnosis, gene analysis, and the treatment of chest infections.

Researchers and paramedics are working hard to develop an accurate and reliable technique for the early diagnosis of COVID-19 to save lives; however, the diagnosis of COVID-19 remains highly idiosyncratic and varies significantly. Therefore, a multi-classification method was created and tested in this work based on deep learning (DL) and a mathematical algorithm model for automatic differentiation of COVID-19 cases from pneumonia based on chest x-ray images. These two diseases were diagnosed using a hybrid model named FPDCnet, which integrates a convolutional neural network (CNN) and Fractional Partial Differential models.

This manuscript has been structured as follows: the materials & methods used are presented in Section 2; the extensive experimental results and their discussion

are in Section 3; the study's conclusion and future work are in Section 4.

2. The Proposed Model

Image enhancement plays a crucial role in improving the quality of medical images by applying algorithms that enhance contrast and highlight fine structural details. In this study, a new and robust deep learning framework, FPDCNet, was designed for the accurate classification of COVID-19 and pneumonia cases from chest X-ray images. The effectiveness of such models depends

heavily on the choice of datasets; therefore, two distinct datasets, one comprising pneumonia cases and the other COVID-19 cases, were carefully selected and subsequently merged before the pre-processing stage. This integration ensures sufficient diversity and representation of infection patterns. The proposed FPDCNet model was then trained to discriminate between normal and abnormal cases, and it achieved reliable detection performance. The overall structure and workflow of the FPDCNet architecture are presented in Figure 1.

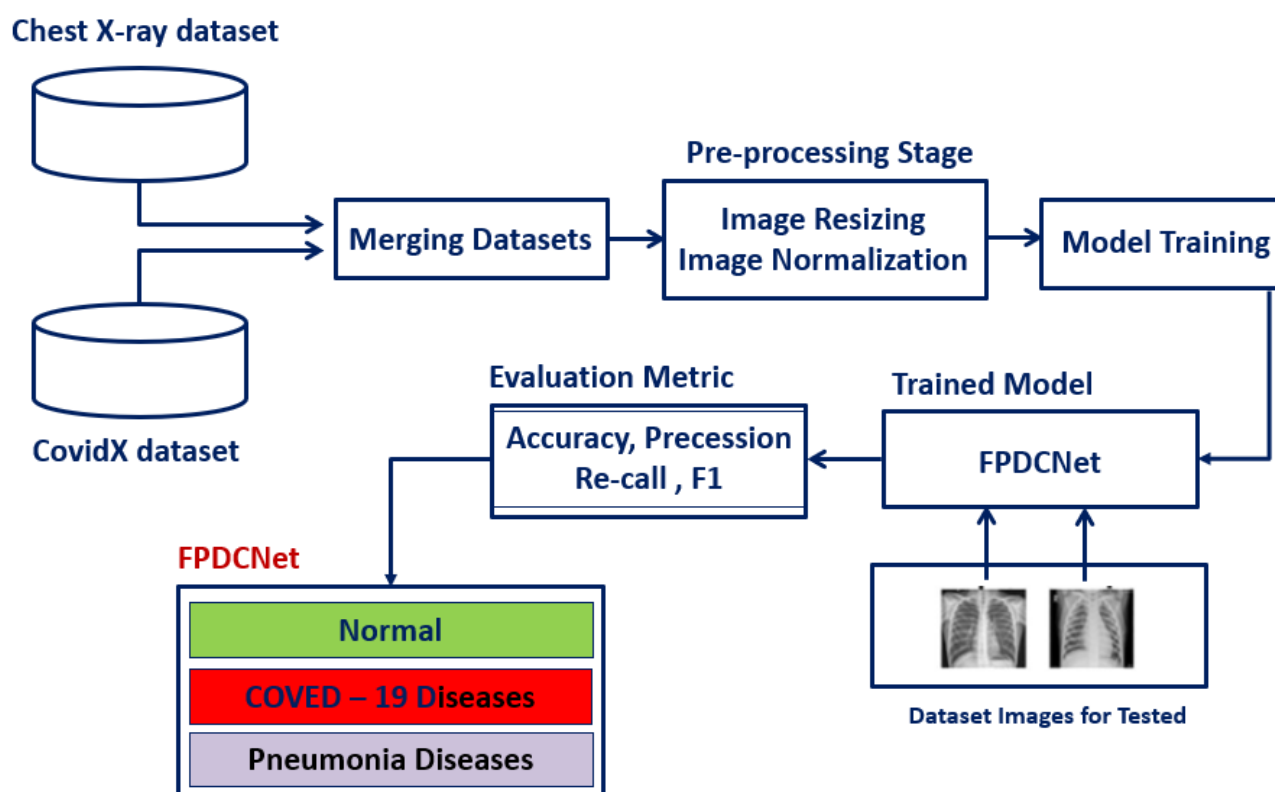


Figure 1. The architecture of the proposed FPDCNet model

2.1. Dataset

Two distinct datasets were employed in this study, one related to pneumonia and the other to COVID-19. The Mendeley Data repository provided the pneumonia dataset, also known as the Chest X-ray dataset, which includes 5,856 chest X-ray pictures [15]. The dataset was divided into the Normal class and the Pneumonia class. Sets for testing, validation, and training are further segmented into each category. The Normal class, in particular, has 1,341 training, 8 validation, and 234 testing images, whereas the Pneumonia class has 3,875 training, 8 validation, and 390 testing images combined. The proposed FPDCNet model for the identification and classification of COVID-19 infections from X-ray images was trained concurrently using the COVID-19 dataset.

There are 13,975 images in the dataset, making it the largest chest X-ray database that is commonly available for COVID-19 research [16].

2.2. Dataset Merging

Before the data pre-processing phase, the two datasets (chest X-rays and COVID-19) were merged; the merging of the two datasets typically uses operations similar to grouping operations. This process combines all records from both datasets, including duplicate records. Equation 1 illustrates the process of merging the two datasets.

$$\text{Merged Dataset} = \text{Pneumonia dataset} \cup \text{COVID-19 dataset} \quad (1)$$

The merge function takes the two datasets as inputs and combines them according to a key column. The general formula can be written as shown in Equation (2).

$$\text{Merged Dataset} = \text{merge}(D_1, D_2, \text{on} = \text{key}, \text{how} = \text{join_type})$$

(2)

Where:

- D_1
 - = Chest X-ray dataset
- D_2
 - = COVID-19 dataset
- key
 - = Common Column (e.g., patient_id)
- how
 - = Join type (inner , outer , left , right)

2.3. Data Prepressing

Data pre-processing is an essential step that must be completed before applying any machine learning or deep learning model. This stage ensures that the acquired data is both high in quality and suitable for model implementation. In this study, the pre-processing procedure consisted of two main steps. The chest X-ray images initially varied in size, with widths ranging from 1350 to 2800 pixels and heights from 690 to 1340 pixels. To maintain consistency, all images were resized to a fixed resolution of 299 × 299 pixels (see Equation 3)[17]. As shown in Table 1, the number of COVID-19 training and validation images was comparatively lower than that of other chest diseases. To address this imbalance,

the “Synthetic Minority Oversampling Technique (SMOTE)” was applied to the utilized X-ray images. SMOTE mitigates the issue of overfitting [18] by generating synthetic samples based on the CNN algorithm. Specifically, it selects random data points from the minority classes and synthesizes new instances. Additionally, data normalization was performed to standardize the input for effective model training[14]. Among the available normalization methods (see Equation 4), pixel normalization was chosen to prepare the data for training the proposed FPDCNet model. After completing these steps, the datasets were ready for the training phase.

$$\text{resized image} = \text{resize}(\text{image}, (299, 299)) \quad (3)$$

$$X' = \frac{X - \mu}{\sigma + \epsilon} \quad (4)$$

Where:

- X'
 - = Normalize pixel value (the output)
- X
 - = The pixel value (for grayscale) images
- μ
 - = mean (average) of pixel values
- σ
 - = Standard deviation of the pixel value
- ϵ
 - = a very small constant (10^{-8}) just to avoid division by zero

Table 1. Splitting of the dataset for training, testing, and validation

Data Splitting	COVID-19	Pneumonia	Normal	Total
Training	1670	2707	2065	6442
Validation	467	773	589	1829
Testing	234	387	295	916
Total	2371	3867	2949	9187

2.4. Training Environment

The “Adam Optimizer” [19] and the “Categorical cross-entropy loss function” [20] are used to train the model. The model was evaluated using different metrics such as precision, F1-score, recall, and accuracy during the

training phase. To minimize overfitting, callbacks such as ModelCheckpoint [21], EarlyStopping [22], and ReduceLROnPlateau [23] routines are also used. ModelCheckpoint serves in saving the model with the best performance during training, while the task of

regularly checking the training accuracy is performed by the EarlyStopping function. The training procedure is terminated if, after a predetermined number of epochs, the accuracy does not increase. The role of the ReduceLROnPlateau function is to reduce the learning rate if the accuracy does not increase after a predetermined number of epochs (the patience parameter is set to 1 in this case). This implies that the learning rate will drop if the accuracy does not increase after one period. Additionally, if there is no improvement in accuracy after 3 epochs, training will be stopped as the stop parameter is set to 3. Now that the factor parameter is set to 0.5, if no improvement is seen after one epoch, the learning rate will be reduced by a factor of 0.5.

2.5. Evaluation Metrics

To evaluate the proposed model, Several metrics have been used to ensure that the proposed FPDCNet is accurate and robust to accurately identify COVID-19 and pneumonia diseases; these metrics have been usually used in the existing studies [14], [24] :

$$Accuracy = \frac{TN + TP}{TN + TP + FN + FP} \quad (5)$$

$$Precision = \frac{TP}{TP + FP} \quad (6)$$

$$Recall = \frac{TP}{TP + FN} \quad (7)$$

$$F - Measure = 2 \frac{Precision \cdot Recall}{Precision + Recall} \quad (8)$$

3. Results And Discussion

3.1. Experimental Results

The achieved results of the proposed FPDCNet model suggest that it is a highly reliable model for automatically detecting COVID-19 and Pneumonia from chest X-ray images. The model's performance was evaluated through training and testing using various evaluation metrics. During the training process, the evaluation process is essential to make sure that the model is functioning smoothly and that adjustments are made accordingly. This section discusses the results that were achieved, followed by a comparison of the proposed model's performance with that of other similar studies. The accuracy variation on the training and validation datasets is depicted in Figure 2, where it begins to rise quickly after 2.5 epochs, peaking after 17 epochs at 0.98.

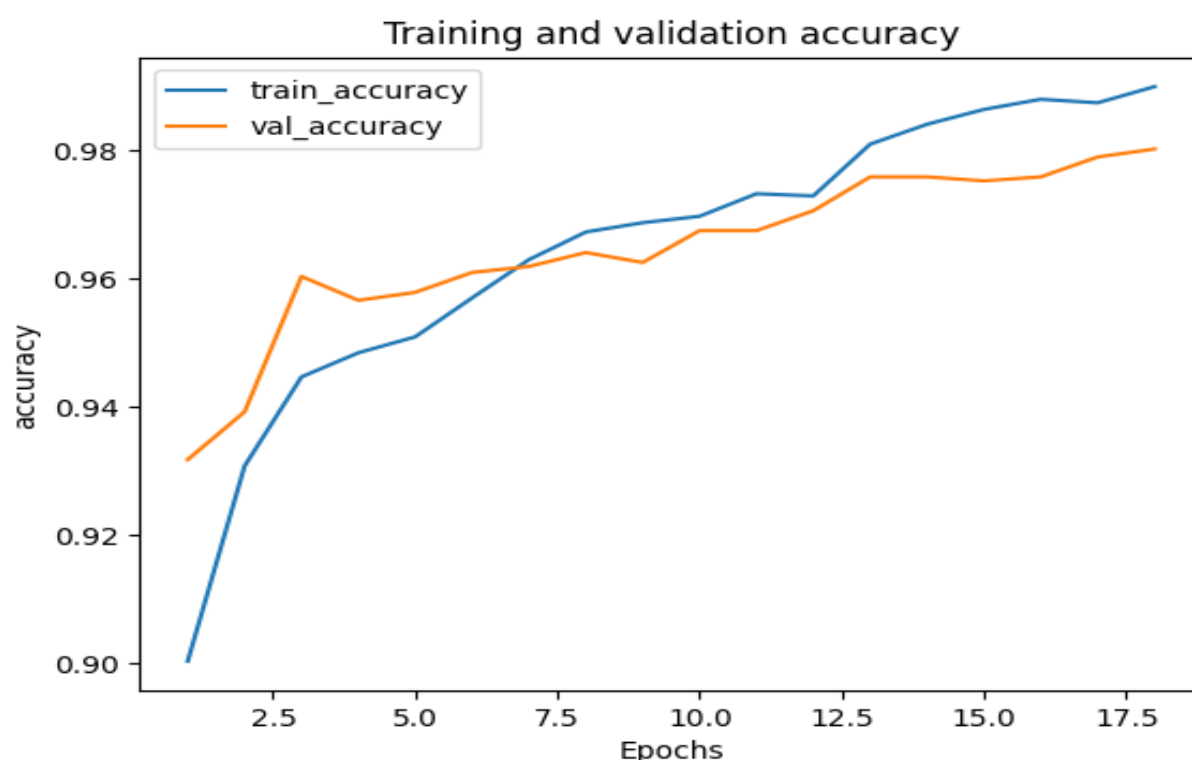


Figure 2. The accuracy metric for the training and validation phases

Figure 3 shows the change in loss over the training and validation phases. As validation progresses, the loss begins to decline but reaches a minor high between 6

and 7.5 epochs before hitting 0.08. However, throughout training, the loss progressively drops until it hits 0.05 after roughly 17 epochs.

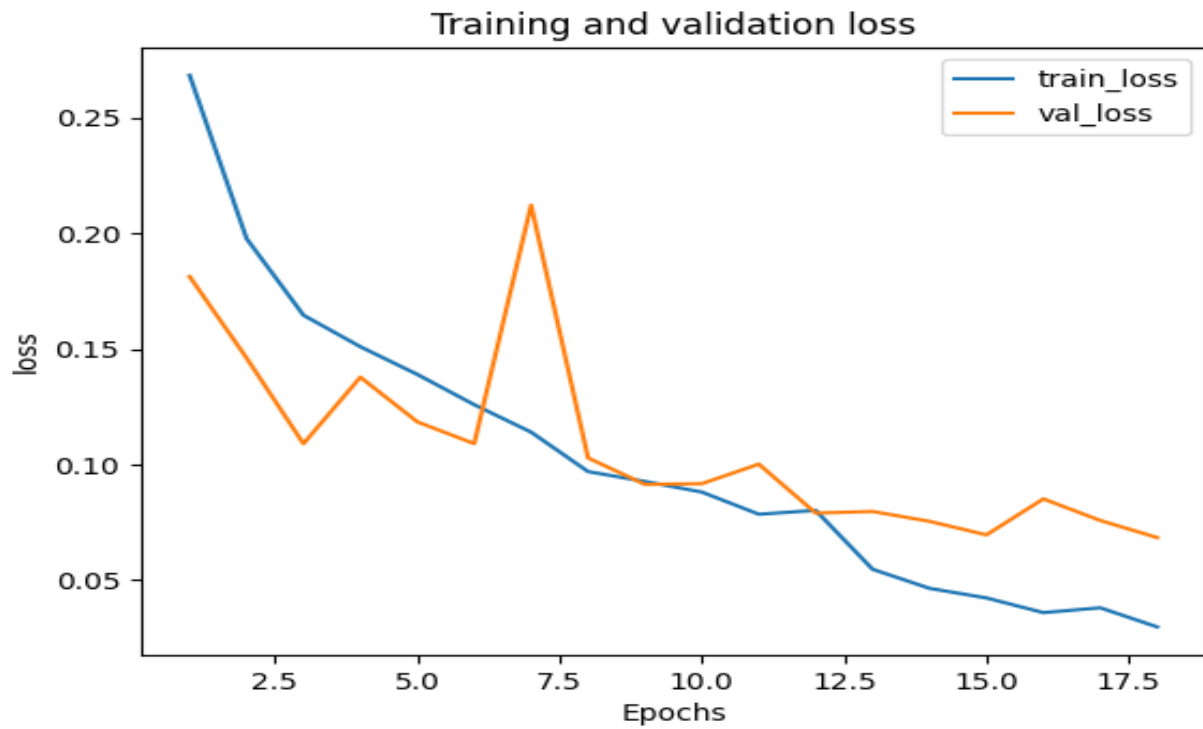


Figure 3. The loss metric for the training and validation phases

Figure 4 depicts the fluctuation of the F1-value; the F1 the training F1 score is higher than the validation F1 score begins to gradually rise in both training and score. validation, reaching its peak after 17 epochs. In the end,

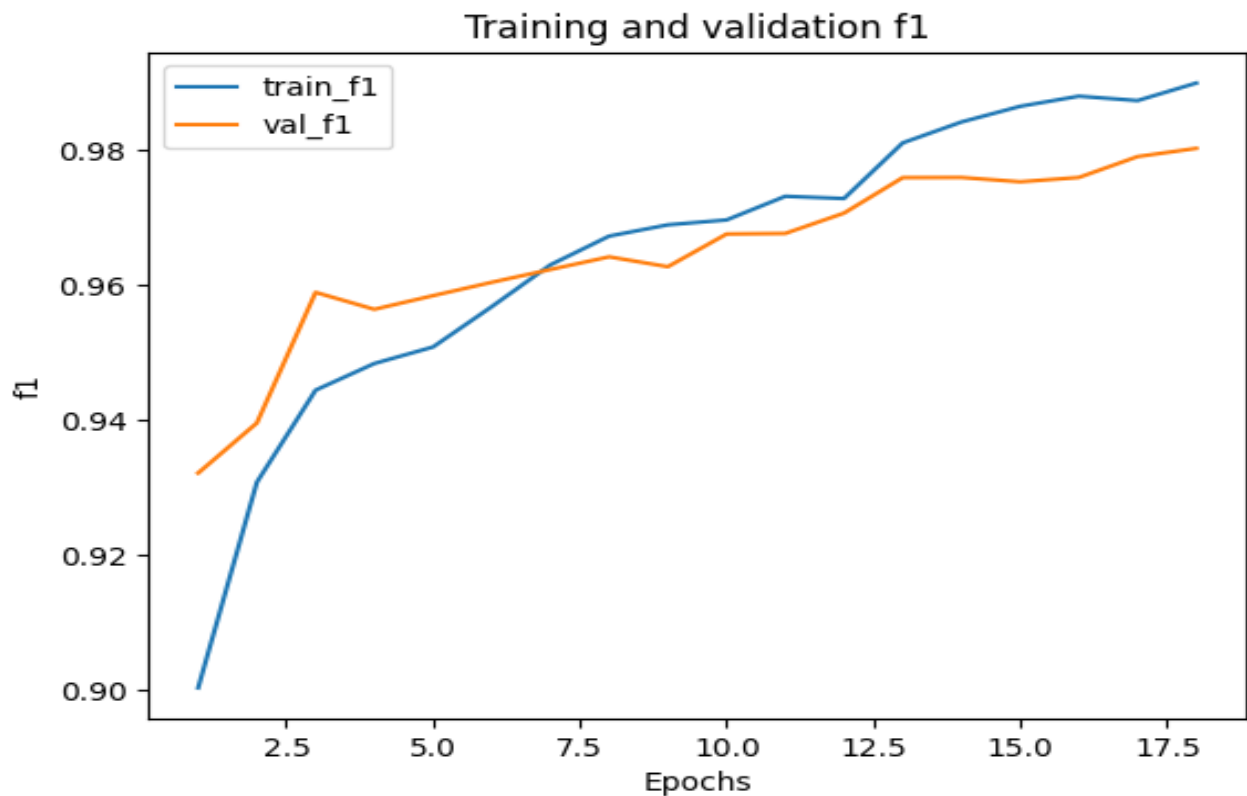


Figure 4. The F1 metric for the training and validation phases

The recall values for the training and validation phases shown in Figure 5 started increasing gradually until the number of epochs was 17.

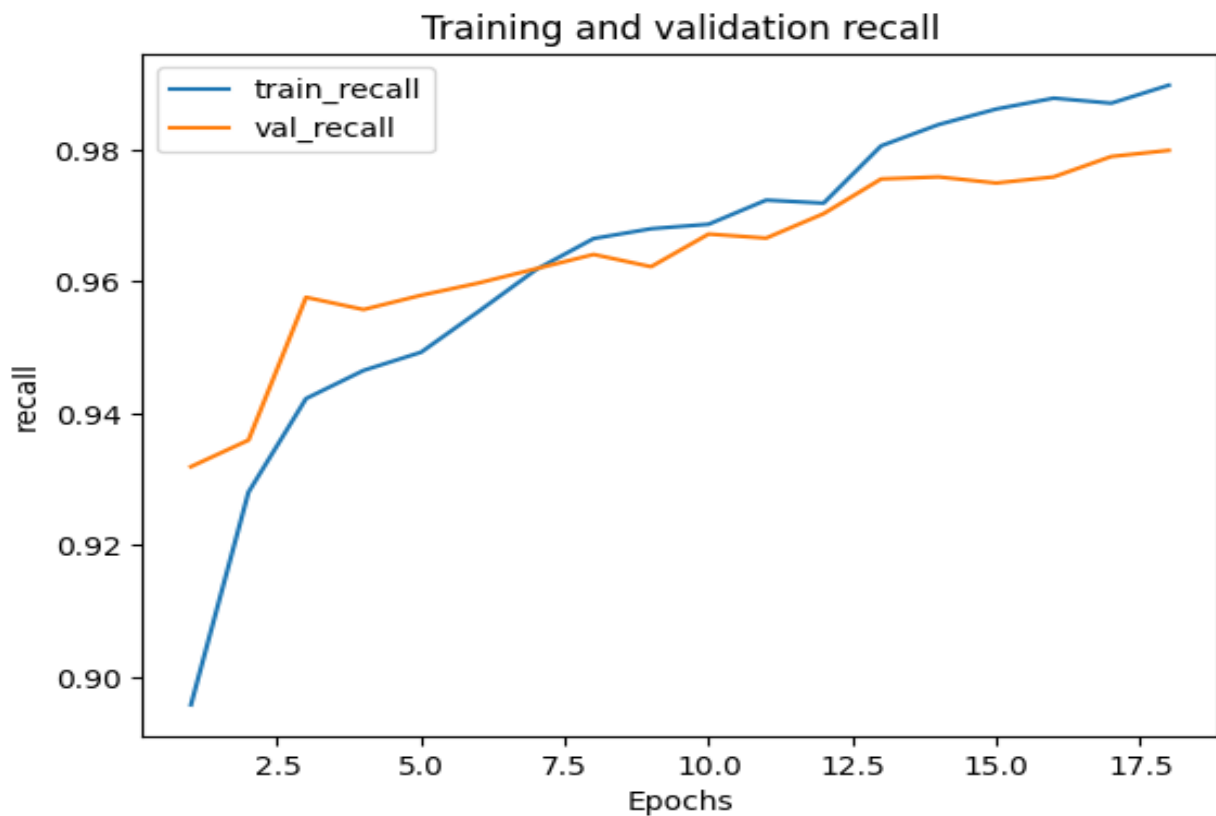


Figure 5. The recall metric for the training and validation phases

The precision value in Figure 6 showed an increment in the training and validation steps, reaching a peak at 17 epochs.

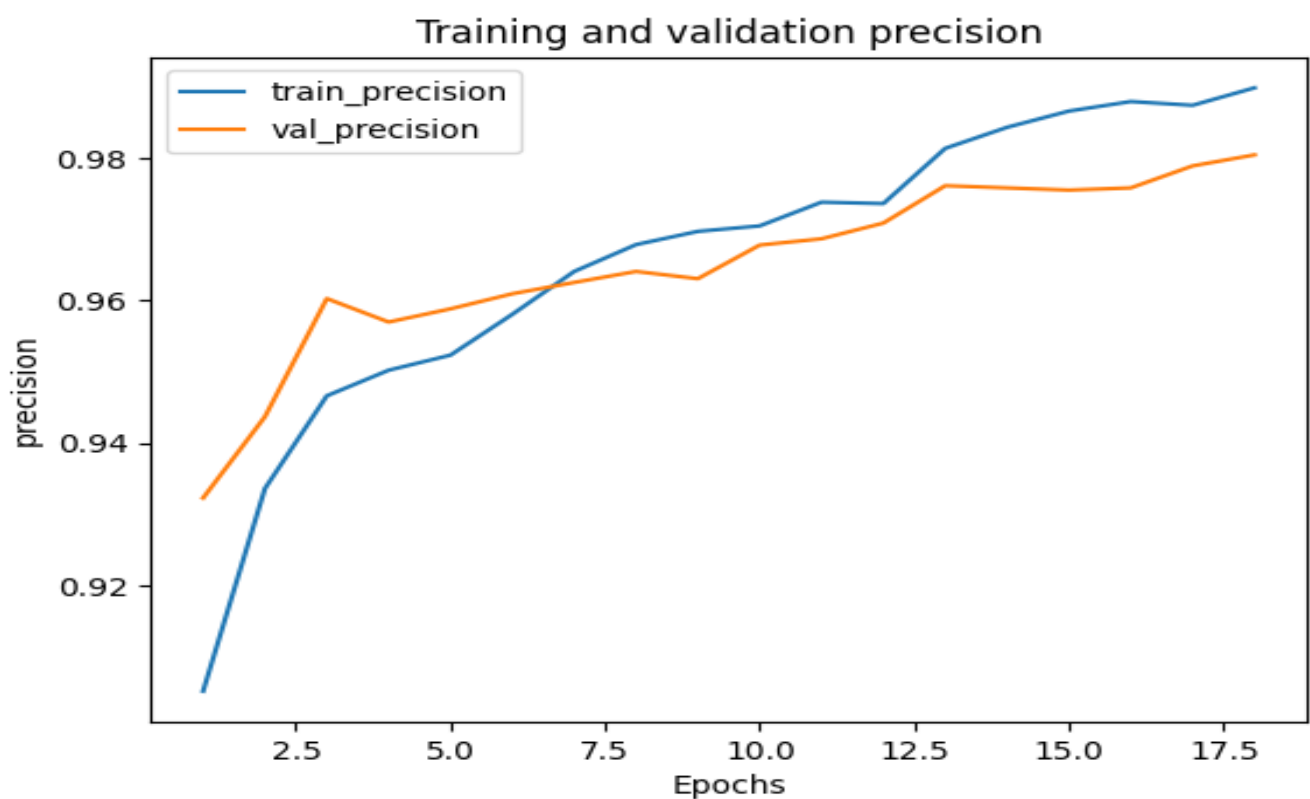


Figure 6. The precision metric for the training and validation phases

3.2. Comparative Study

The FPDCNet model was selected for this investigation due to its outstanding characteristics and capability for

producing high-quality classification results. Nevertheless, a number of studies have used deep learning models to categorize pneumonia and COVID-

19. The performance of the two previous models is summarized and contrasted with the suggested FPDCNet model in this section. Using a VGG model, the first models [25] recorded 97.13 %, 96.48 %, and 96.89 % accuracy values during the testing, validation, and training phases, respectively. In this study, the specific results for each class showed an accuracy value of 98.19 % for bacterial pneumonia, 97.67 % for COVID-19, and 97.93 % for the normal class. Hence, the FPDCNet model is an appropriate and better model for the accurate categorization of COVID-19 and pneumonia cases.

In the second investigation [26], a pre-trained CNN architecture with the VGG-16 and DenseNet121 models was used. The CNN model performed better than the pre-trained networks in terms of F1-score, recall, and precision. Furthermore, compared to the pre-trained networks' accuracy rate of 88 %, the CNN model's accuracy rate of 91 % was significantly better. Figure 7 shows that, in comparison to the two experiments mentioned, the suggested FPDCnet model in this study achieved the maximum accuracy of 98.10 %. Figure 7 shows the accuracy comparison between the proposed model and the referenced models.

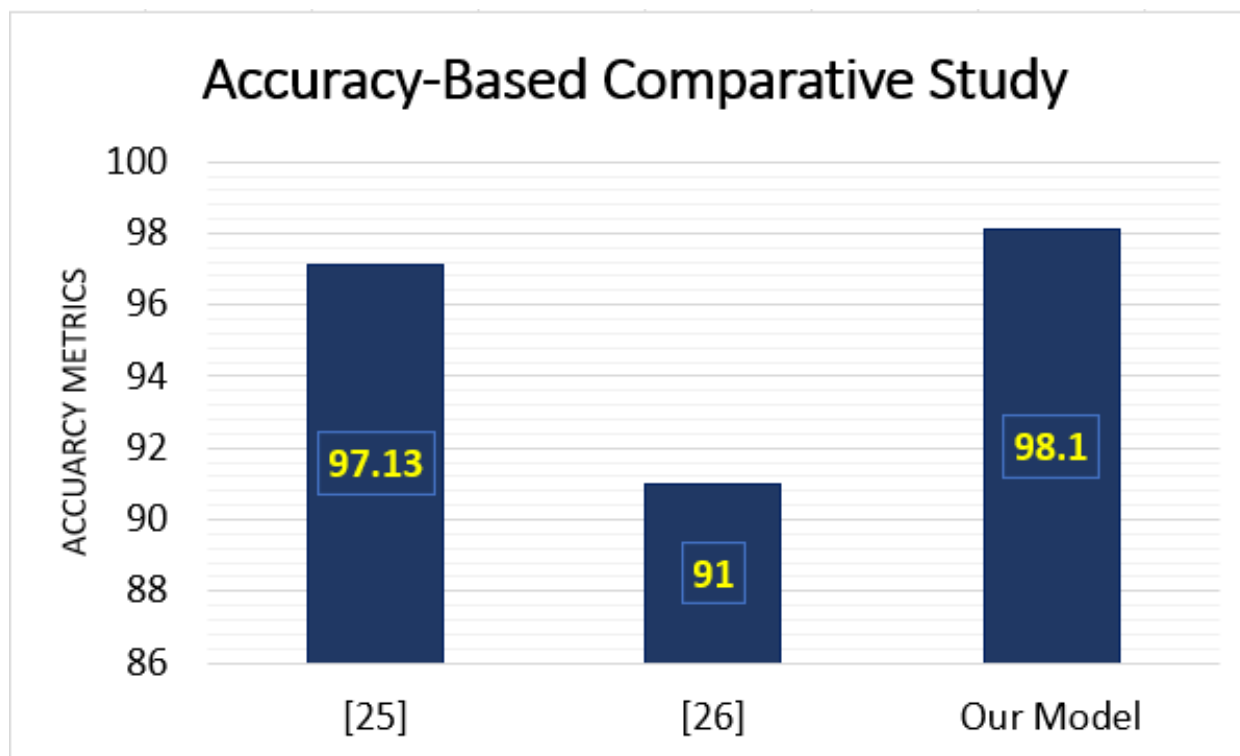


Figure 7. A comparison analysis of the accuracy of the proposed model and the referenced models

4. Conclusion And Future Direction

Following the outbreak of the COVID-19 pandemic and its severe health consequences, the urgent need to rapidly and accurately detect COVID-19 infections became evident. As medical understanding of the disease advanced, differentiating COVID-19 from pneumonia gained critical importance since both conditions require distinct diagnostic and treatment approaches. In response, a large body of research has been dedicated to developing intelligent models that can effectively distinguish between normal cases, pneumonia cases, and COVID-19 infections using chest X-ray images. In this study, a hybrid framework that integrates deep learning with advanced mathematical modelling was introduced and named the FPDCnet **model**. By embedding fractional partial differential (FPD) operators into the convolutional layers of the CNN

architecture, the model leverages both feature extraction and fractional-order dynamics to enhance classification performance. The proposed model demonstrated remarkable results, achieving a precision of 0.982 and an accuracy of 98.1 % in distinguishing between the three classes (normal, pneumonia, and COVID-19). These findings confirm that the proposed FPDCnet model is a powerful diagnostic tool with strong potential for supporting medical decision-making in real-world clinical settings.

4.1. Future Directions

While the current model exhibits high performance, the integration of fractional-order algorithms offers vast opportunities for future development in medical imaging and beyond. Unlike classical integer-order methods, fractional partial differential equations

(FPDEs) allow for modelling memory and hereditary properties in data, which is particularly useful for representing the complex dynamics of biological systems. A general form of the time–space fractional diffusion equation that could be embedded into future AI architectures is:

$$\frac{\partial^\alpha v(x, \tau)}{\partial t^\alpha} = D \frac{\partial^\beta v(x, \tau)}{\partial |x|^\beta} + f(v(x, \tau)).$$

Where:

- $\alpha \in (0,1]$ represents the fractional order in time (capturing memory effect)
- $\beta \in (0,2]$ represents the fractional spatial derivative (capturing long-range dependencies)
- D is the diffusion coefficient
- $f(v(x, \tau))$ model nonlinear dynamics such as disease progression

By embedding such equations into CNNs, future models could dynamically adapt feature extraction to temporal-spatial patterns in medical images. This may significantly improve not only COVID-19 and pneumonia detection but also broader applications such as cancer screening, neurodegenerative disease monitoring, and real-time epidemic modelling.

References

1. T. Gheit, B. Abedi-Ardekani, C. Carreira, C. G. Missad, M. Tommasino, and M. C. Torrente, "Comprehensive analysis of HPV expression in laryngeal squamous cell carcinoma," *J. Med. Virol.*, vol. 86, no. 4, pp. 642–646, 2014.
2. V. Carlini *et al.*, "The multifaceted nature of IL-10: regulation, role in immunological homeostasis and its relevance to cancer, COVID-19 and post-COVID conditions," *Front. Immunol.*, vol. 14, p. 1161067, 2023.
3. I. M. Artika, Y. P. Dewi, I. M. Nainggolan, J. E. Siregar, and U. Antonjaya, "Real-time polymerase chain reaction: current techniques, applications, and role in COVID-19 diagnosis," *Genes (Basel)*, vol. 13, no. 12, p. 2387, 2022.
4. G. D. Sharma, A. K. Tiwari, M. Jain, A. Yadav, and M. Srivastava, "COVID-19 and environmental concerns: A rapid review," *Renew. Sustain. Energy Rev.*, vol. 148, p. 111239, 2021.
5. A. Tahamtan and A. Ardebili, "Real-time RT-PCR in COVID-19 detection: issues affecting the results," *Expert Rev. Mol. Diagn.*, vol. 20, no. 5, pp. 453–454, 2020.
6. V. M. Corman, "Detection of 2019 novel coronavirus (2019-nCoV) by real-time RT-PCR. Euro Surveill.," (No Title), vol. 25, no. 3, 2020.
7. C. Bezier, G. Anthoine, and A. Charki, "Reliability of real-time RT-PCR tests to detect SARS-Cov-2: A literature review," *Int. J. Metrol. Qual. Eng.*, vol. 11, p. 13, 2020.
8. S. Resnick *et al.*, "Clinical relevance of the routine daily chest X-ray in the surgical intensive care unit," *Am. J. Surg.*, vol. 214, no. 1, pp. 19–23, 2017.
9. A. Komal and H. Malik, "Transfer learning method with deep residual network for COVID-19 diagnosis using chest radiographs images," in *Proceedings of International Conference on Information Technology and Applications: ICITA 2021*, Springer, 2022, pp. 145–159.
10. A. N. Zakirov, R. F. Kuleev, A. S. Timoshenko, and A. V. Vladimirov, "Advanced approaches to computer-aided detection of thoracic diseases on chest X-rays," *Appl Math Sci*, vol. 9, no. 88, pp. 4361–4369, 2015.
11. B. F. King, "Artificial intelligence and radiology: what will the future hold?," *J. Am. Coll. Radiol.*, vol. 15, no. 3, pp. 501–503, 2018.
12. A. Davila, J. Colan, and Y. Hasegawa, "Comparison of fine-tuning strategies for transfer learning in medical image classification," *Image Vis. Comput.*, vol. 146, p. 105012, 2024.
13. R. Kumar, P. Kumbharkar, S. Vanam, and S. Sharma, "Medical images classification using deep learning: a survey," *Multimed. Tools Appl.*, vol. 83, no. 7, pp. 19683–19728, 2024.
14. S. A. Schnawa, M. Rafie, and M. S. Taha, "DAE-DBN: An Effective Lung Cancer Detection Model Based on Hybrid Deep Learning Approaches," in *International Conference of Reliable Information and Communication Technology*, Springer, 2023, pp. 108–118.
15. D. Kermany, K. Zhang, and M. Goldbaum, "Large dataset of labeled optical coherence tomography (oct) and chest x-ray images," *Mendeley Data*, vol. 3, no. 10.17632, 2018.
16. E. Hassan, M. Y. Shams, N. A. Hikail, and S. Elmougy, "COVID-19 diagnosis-based deep learning approaches for COVIDx dataset: A preliminary survey," *Artif. Intell. Dis. Diagnosis Progn. Smart Healthc.*, vol. 107, 2023.

17. N. A. Yaseen, A. A.-A. Hadad, and M. S. Taha, "An Anomaly Detection Model Using Principal Component Analysis Technique for Medical Wireless Sensor Networks," in *2021 International Conference on Data Science and Its Applications (ICoDSA)*, IEEE, 2021, pp. 66–71.
18. A. A.-A. Hadad, H. N. Khalid, Z. S. Naser, and M. S. Taha, "A Robust Color Image Watermarking Scheme Based on Discrete Wavelet Transform Domain and Discrete Slantlet Transform Technique," *Ing. des Syst. d'Information*, vol. 27, no. 2, p. 313, 2022.
19. A. S. Ahmed, A. A.-A. Haddad, R. S. Hameed, and M. S. Taha, "An Accurate Model for Text Document Classification Using Machine Learning Techniques," *J. homepage <http://iieta.org/journals/isi>*, vol. 30, no. 4, pp. 913–921, 2025.
20. Y. Ho and S. Wookey, "The real-world-weight cross-entropy loss function: Modeling the costs of mislabeling," *IEEE access*, vol. 8, pp. 4806–4813, 2019.
21. F. D. Schmidt, I. Vulić, and G. Glavaš, "Free Lunch: Robust Cross-Lingual Transfer via Model Checkpoint Averaging," *arXiv Prepr. arXiv2305.16834*, 2023.
22. M. V. Ferro, Y. D. Mosquera, F. J. R. Pena, and V. M. D. Bilbao, "Early stopping by correlating online indicators in neural networks," *Neural Networks*, vol. 159, pp. 109–124, 2023.
23. A. Al-Kababji, F. Bensaali, and S. P. Dakua, "Scheduling techniques for liver segmentation: Reducelronplateau vs onecyclelr," in *International Conference on Intelligent Systems and Pattern Recognition*, Springer, 2022, pp. 204–212.
24. H. A. Alrikabi, W. Annajjar, A. M. Alnasrallah, S. T. Mustafa, and M. S. M. Rahim, "Using FFNN Classifier with HOS-WPD Method for Epileptic Seizure Detection," in *2019 IEEE 9th International Conference on System Engineering and Technology (ICSET)*, IEEE, 2019, pp. 360–363.
25. S. H. Karaddi, K. Srilakshmi, L. D. Sharma, D. Sharma, and R. S. Singh, "Detection of COVID-19 using CoviNet and VGG-16 Models," in *2023 3rd International conference on Artificial Intelligence and Signal Processing (AISP)*, IEEE, 2023, pp. 1–5.
26. A. P. Shinde, "Multiclass classification of Covid-19, Tb, Pneumonia, and health cases using Deep Learning." Dublin, National College of Ireland, 2022.